Dual-mode humidity detection using a lanthanide-based metal-organic framework: towards multifunctional humidity sensors

Gao, Y.; Jing, P.; Yan, N.; Hilbers, M.; Zhang, H.; Rothenberg, G.; Tanase, S.

DOI
10.1039/C7CC01122A

Publication date
2017

Document Version
Other version

Published in
Chemical Communications

Dual-mode humidity detection using a lanthanide-based metal-organic framework: towards the development of multifunctional humidity sensors

Yuan Gao,[a] Pengtao Jing,[a,b] Ning Yan,[a] Michiel Hilbers,[a] Hong Zhang,[a,b] Gadi Rothenberg,[a] Stefania Tanase[a]*

[a] *Van' t Hoff Institute for Molecular Sciences, University of Amsterdam, Science Park 904, 1098 XH Amsterdam, The Netherlands. E-mail: s.grecea@uva.nl; h.zhang@uva.nl*

[b] *State Key Laboratory of Luminescence and Applications, Changchun Institute of Optics, Fine Mechanics and Physics, Chinese Academy of Sciences, Changchun 130033, P. R. China*

Electronic Supporting Information

Materials and instrumentation

Infrared spectra (4000–400 cm^{-1}, resol. 0.5 cm^{-1}) were recorded on a Varian 660 FTIR spectrometer using KBr pellets and the transmission technique. Powder X−ray diffraction was carried out on a Rigaku Miniflex X-ray Diffractometer. Measurements were done from 3° to 50° with a turning speed of 2.0 °/min. Thermogravimetric analysis (TGA) and differential scanning calorimetry (DSC) were performed using a NETZSCH Jupiter® STA 449F3 instrument. The measurements were done under argon (20 $mlmin^{-1}$) at 35–800 °C. Unless stated otherwise, all chemicals were commercially available (Aldrich, >99% pure) and used as received. The $K_4[M(CN)_8]\cdot 2H_2O$ (M^{4+} = W, Mo) precursors and the EuM MOFs were synthesized as reported previously.[1, 2]

Photophysical measurements

Excitation and emission spectra were recorded on a Perkin Elmer LS50B luminescence spectrometer. Measurements were taken on the as-synthesised EuM MOFs (M = Mo, W) and the EuW MOF activated at 80 °C and then exposed to different relative humidity (RH) conditions (in the measuring chamber). The emission spectra intensity was corrected for the sensitivity of the detector. The humidity environment was controlled using different saturated salt solutions.

Luminescence lifetimes were measured using a tunable Nd:YAG-laser system (NT342B, Ekspla) comprising the pump laser (NL300) with harmonics generators (SHG, THG) producing 355 nm to pump an optical parametric oscillator (OPO) with SHG connected in a single device. The excitation energy of laser was 4 mJ/pulse. The laser beam at sample had a diameter of 5 mm without focusing. The laser system was operated at 10 Hz repetition rate with a pulse length of 5 ns. Emission wavelength was selected using a Carl Zeiss M20 single grating monochromator, and the signal is detected using a Hamamatsu PMT type R928P. The luminescence decay curves were recorded every 60 s using a Tektronix 500 MHz digital oscilloscope (Tektronix PDO4054) and a home-written Labview program.

The sample's stability after each light irradiation measurement is verified by PXRD analysis and also by suspending the sample in water solution. If the burning of the organic portion of the MOFs would occur, this would also result in the formation of free octacyanometallate ions as impurities. Such impurities are very soluble in water and they can be easily identified from the yellow color of the solution or by UV-Vis.

Electrochemical impedance spectroscopy (EIS) measurements.

Samples were prepared using the previous published procedures.[3] The crystalline product was grinded with a mortar and pestle to uniform particle size. The disk-shaped pellets of the EuW MOF were prepared by using a press and a die measuring 13 mm in diameter. The pellet was placed between a pair of parallel copper plates anchored by a clamp. The typical thickness of the sample was ~0.2 mm (±0.05 mm). The electrochemical cell was then fixed with clamp and placed in a humidity-controlled environment which is controlled by different saturated salt solutions. The relative humidity was double checked with the digital sensor. Impedance analysis was measured using 4−points method at different temperatures (30−85 °C) and relative humidities (20−100%).The electrochemical impedance spectroscopy (EIS) tests were carried out under open-circuit voltage (OCV) conditions using a Gamry potentiostat with a frequency range of 10^6 Hz to 0.1 Hz and voltage amplitude of 10 mV. The impedance response and the recovery time to different relative humidity (RH) values, ranging from 100% to 68% were measured at 500 Hz and 10 mV for powder samples of EuW MOF.

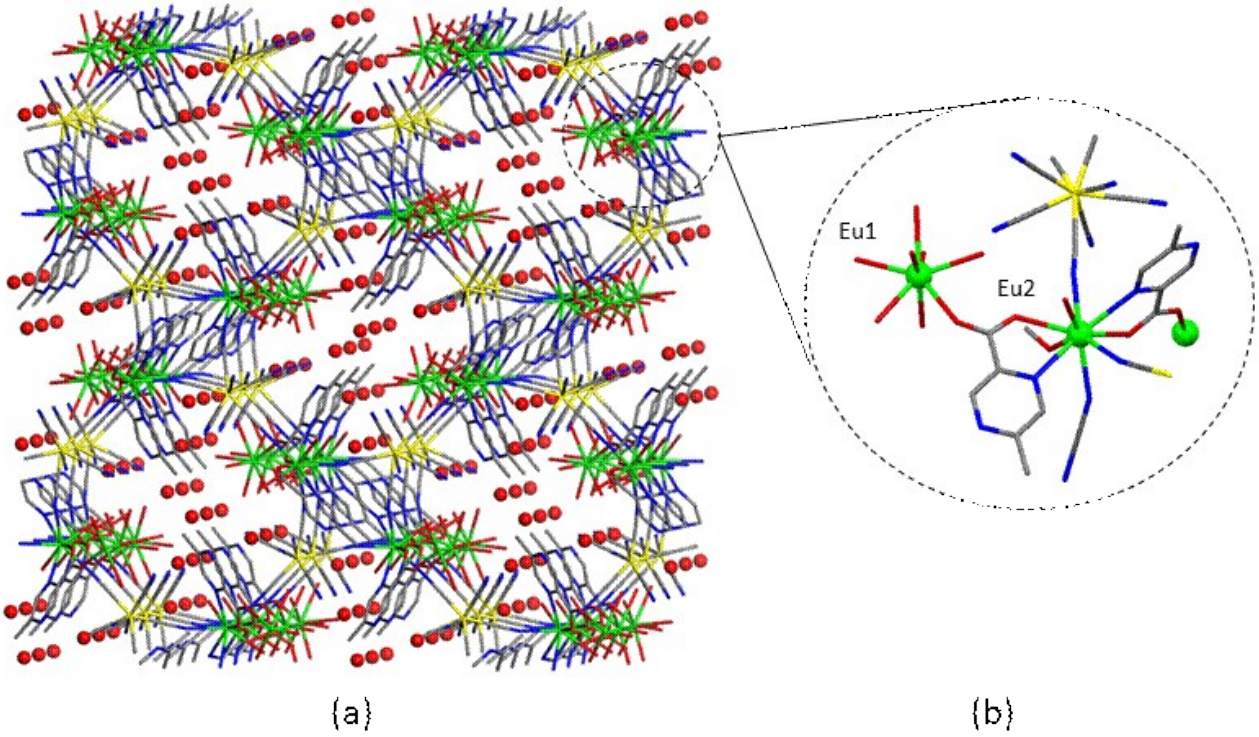

Figure S1. (a) The three-dimensional crystal structure of the EuM MOF viewed along the *b*-axis. (b) Close-up view of a single unit cell showing the different coordination environments of the two Eu^{3+} nodes (Eu1 and Eu2).

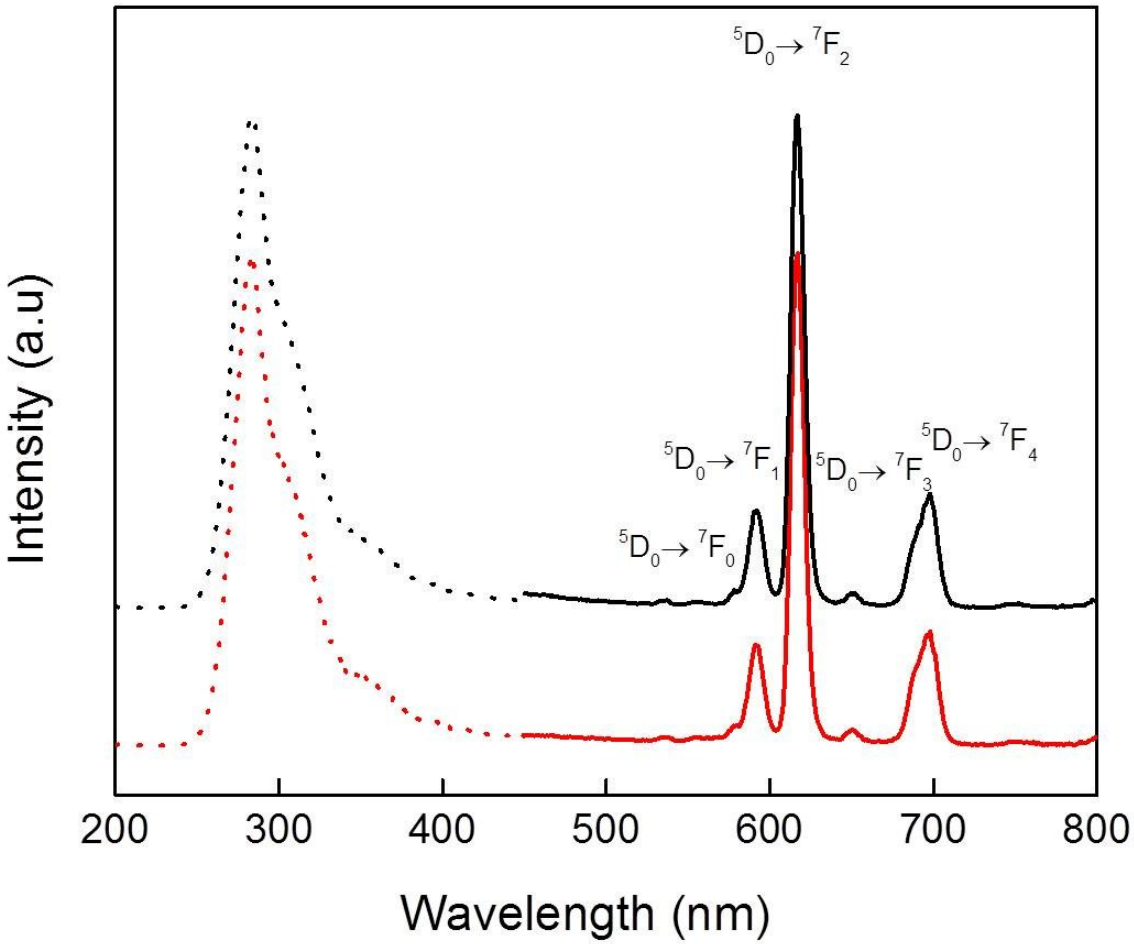

Figure S2. Excitation (λ_{em} = 617 nm, dotted line) and emission (λ_{ex} = 280 nm, continuous line) spectra of EuMo (red) and EuW (black) MOFs at room temperature.

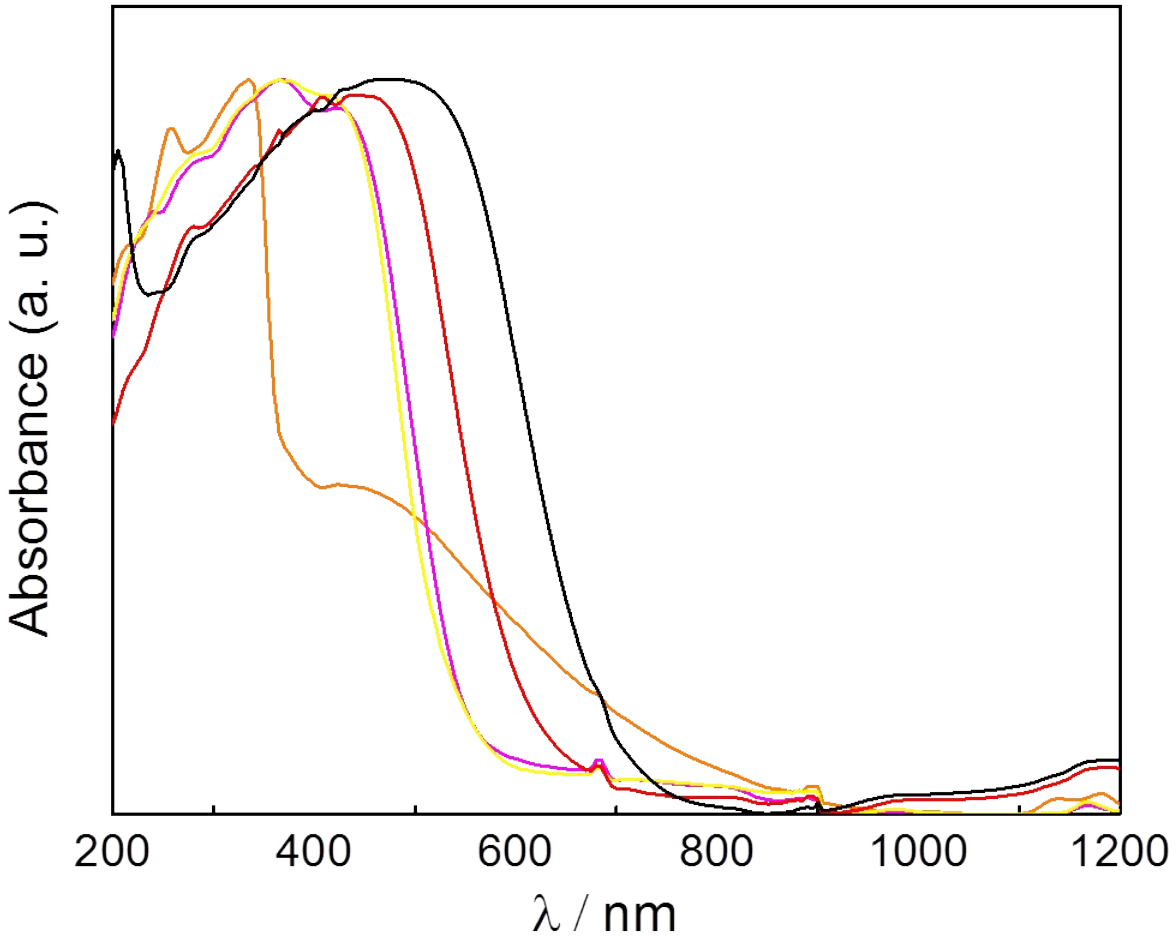

Figure S3. UV-Vis spectra of the EuMo (red) and EuW (black) MOFs, $K_4[Mo(CN)_8]\cdot 2H_2O$ (yellow), $K_4[W(CN)_8]\cdot 2H_2O$ (pink) and the Hmpca ligand (orange).

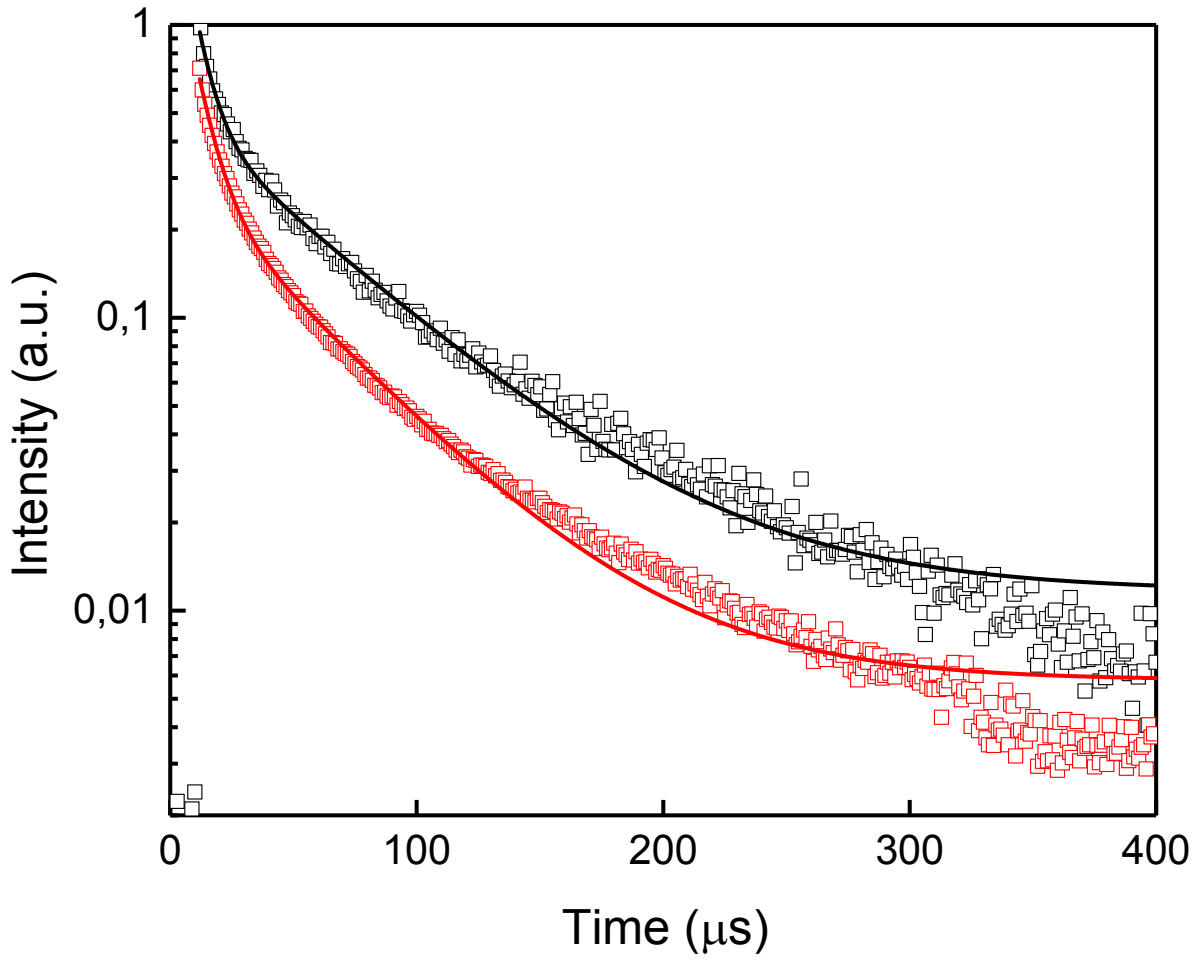

Figure S4. The luminescence decay curves of the $^5D_0 \rightarrow {}^7F_2$ transition in EuMo (red) and EuW (black) MOFs.

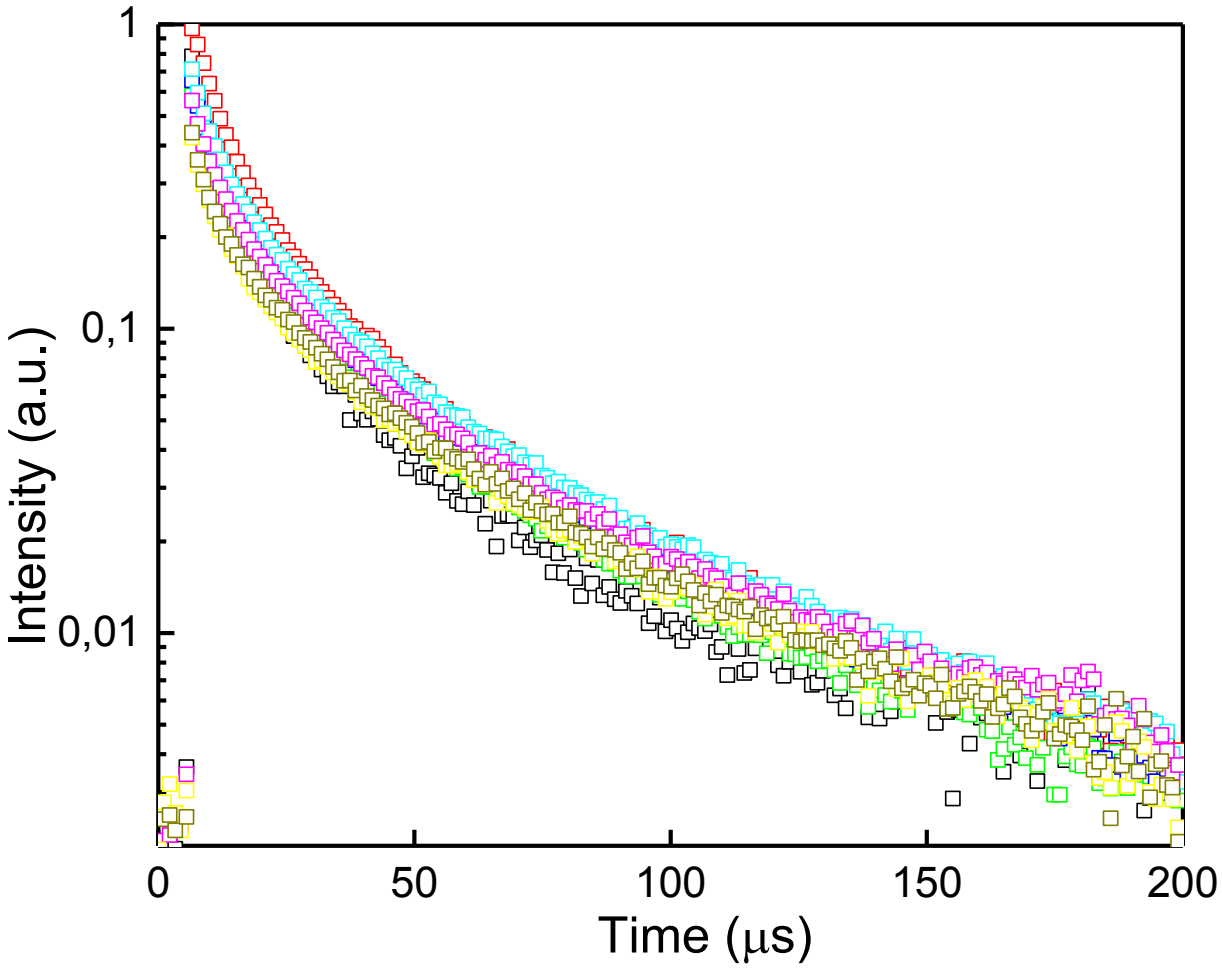

Figure S5. The luminescence decay curves of the $^5D_0 \rightarrow {}^7F_2$ transition in EuMo MOF measured within 16 min.

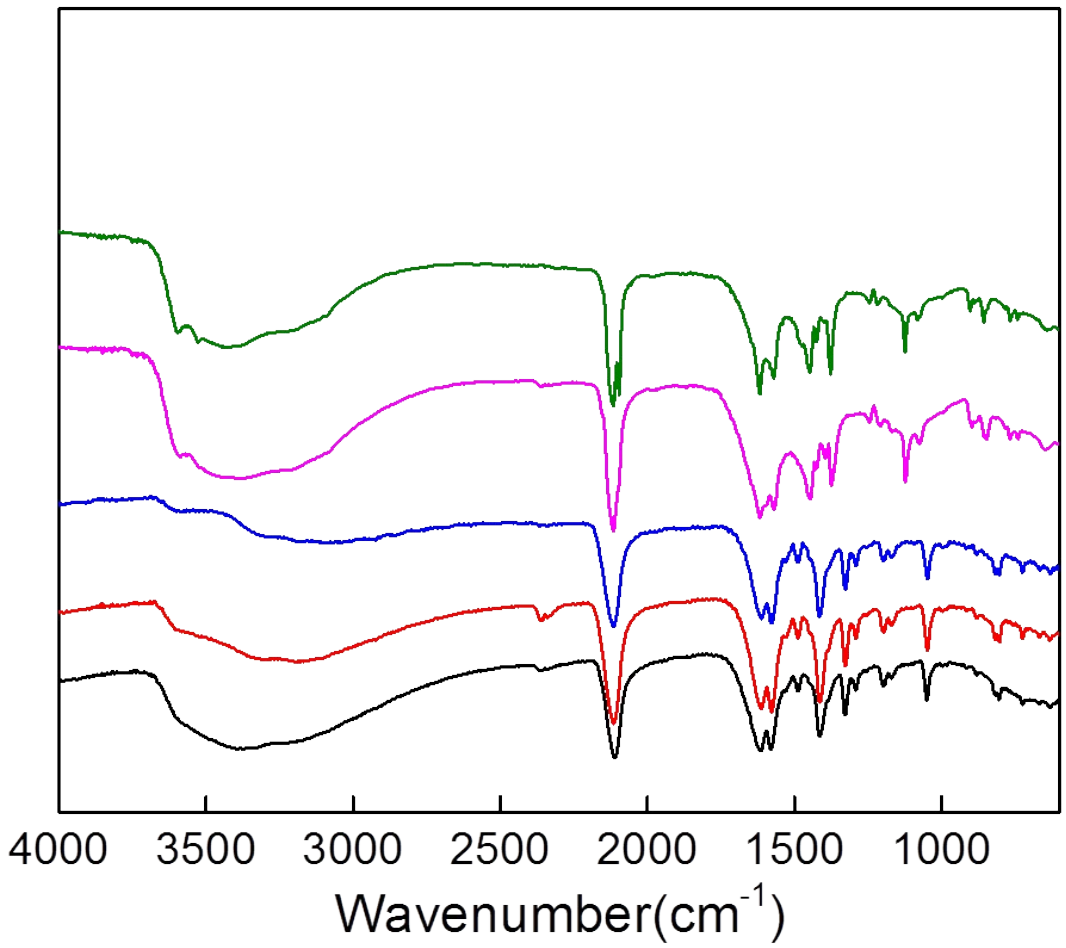

Figure S6. IR spectra of the as-synthesised EuW MOF (black), the EuW MOF activated at 80 °C (red) and its rehydrated form (pink), and the EuW MOF activated at 130 °C (blue) and its rehydrated form (green).

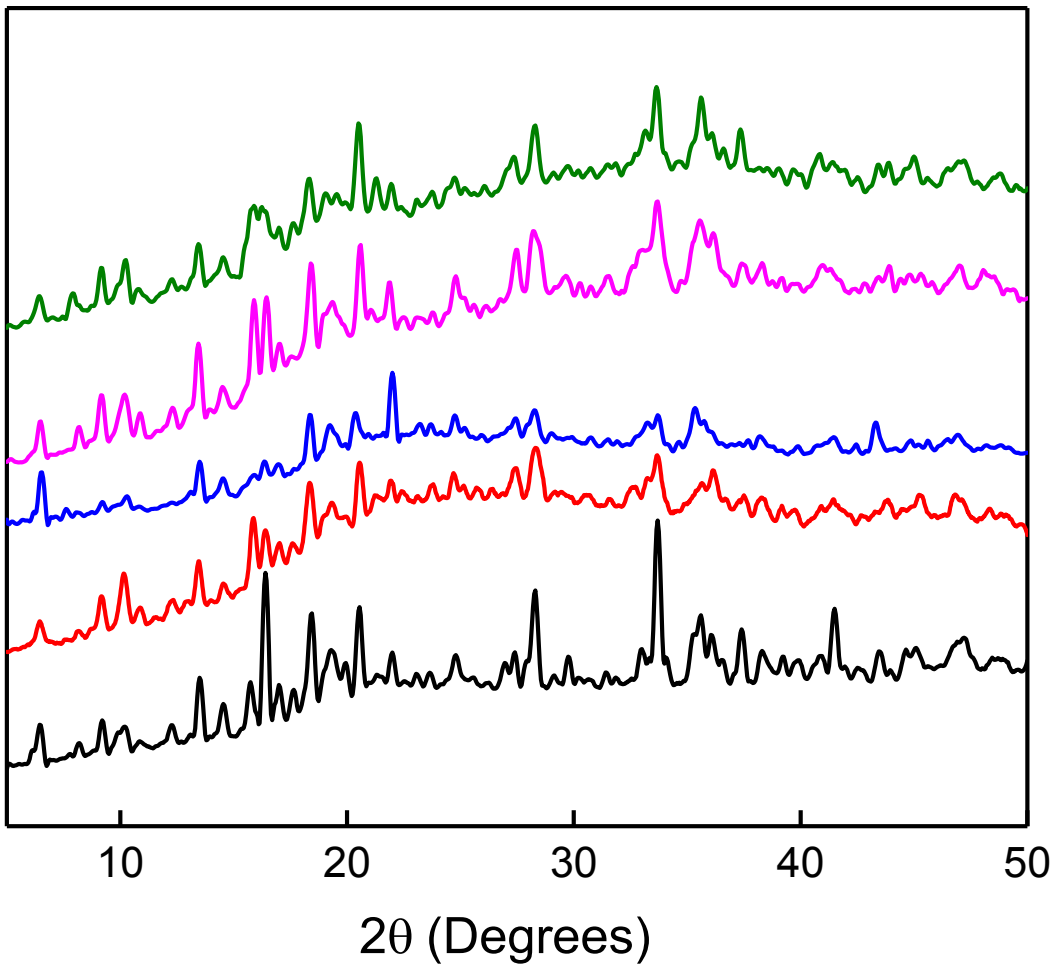

Figure S7. PXRD patterns of the as-synthesised EuW MOF (black), the EuW MOF activated at 80 °C (red) and its rehydrated form (pink), and the EuW MOF activated at 130 °C (blue) and its rehydrated form (green).

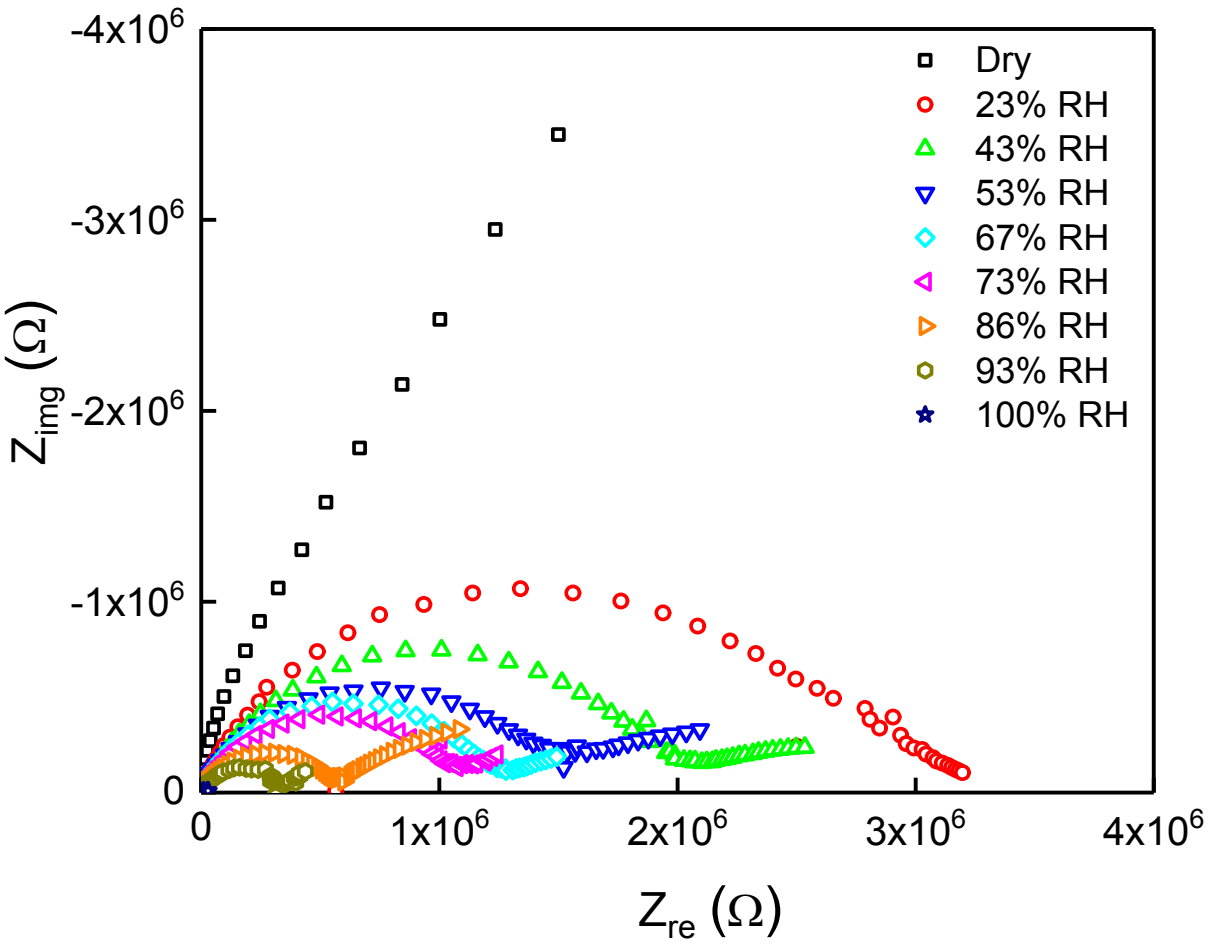

Figure S8. Nyquist plots measured at room temperature and different relative humidities.

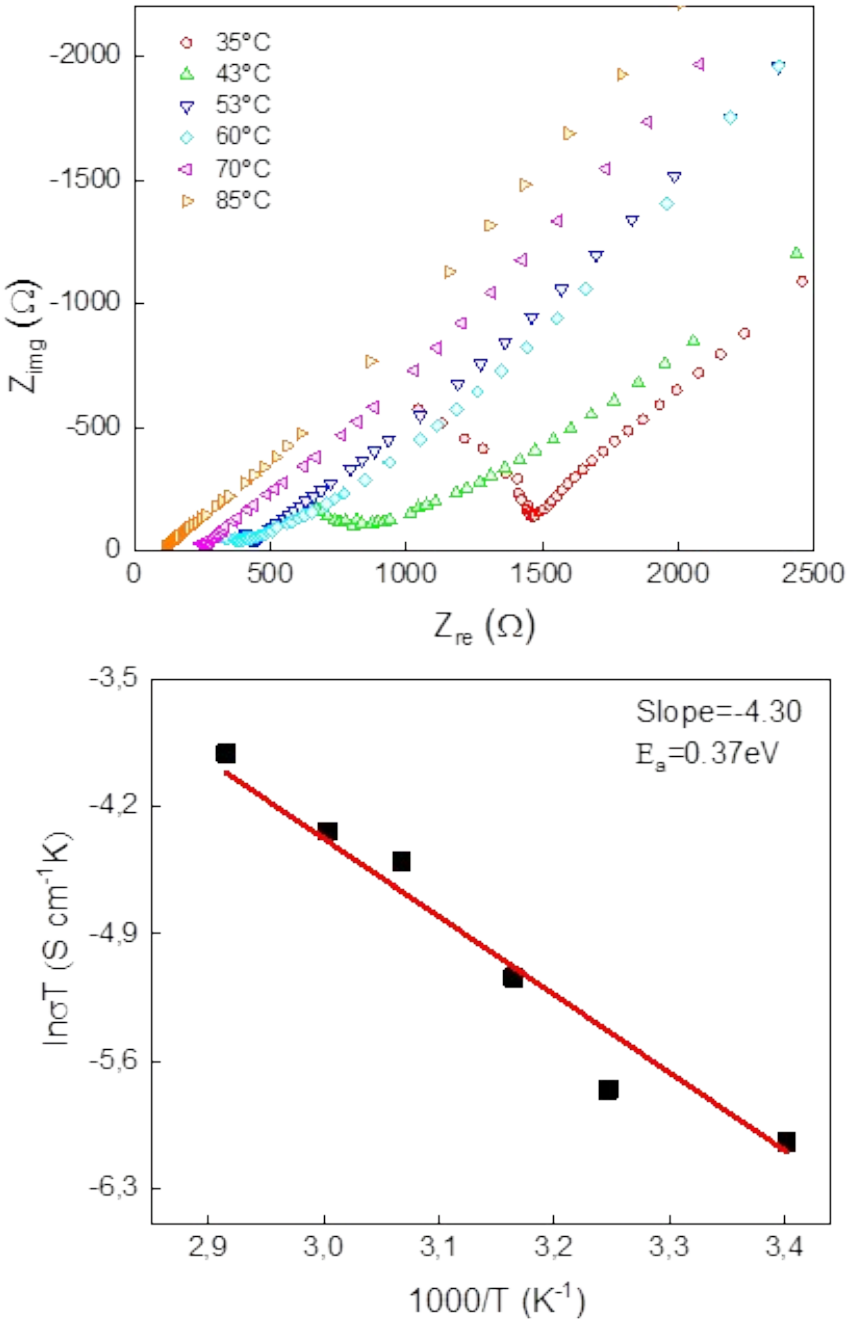

Figure S9. Nyquist plots measured at 100% relative humidity and different temperatures (top) and the corresponding Arrhenius plot (bottom) for the EuW MOF.

Table S1. The response time of lanthanide-based MOFs used for humidity sensing.

Compound	Response time (min)	Recovery time (hours)	Characterization method	Rehydration condition	Reference
$[Eu(H_2O)_2(mpca)_2Eu(H_2O)_6W(CN)_8]\cdot nH_2O$	5	1	Decay time PXRD	Dropwise of water	This work
$[Er_2(fum)_3(H_2O)_4]\cdot 8H_2O$	n.d.	48	TGA	Water vapor	[4]
$Ba_2(H_2O)_4[Eu(L1)_3(H_2O)_2]\cdot(H_2O)_nCl$	~30	1	TGA	Water vapor	[5]
$[Tb_2(BDOA)_3(H_2O)_4]\ 6H_2O$	n.d.	24	PXRD	Soaked in water	[6]
$[Sm_2(fumarate)_3(H_2O)_4]\cdot 3H_2O$	n.d.	24	PXRD	Water vapor	[7]
$[Cu_3(bpy)_2Yb_2(ip)_6]\cdot 5H_2O$	n.d.	24	PXRD	Water vapor	[8]
$[La_2(H_2O)][C_5N_1H_3(COO)_2]_3\cdot 2H_2O$	30	~2	PXRD	Ambient conditions	[9]
$[Ln_2(fum)_2(ox)(H_2O)_4]\ 4H_2O$	n.d.	24	PXRD	Water vapor	[10]
$[Gd_2(H_2O)_2Ni(H_2O)_2(bdc)_2(2,5\text{-}pydc)_2]_3\cdot 8H_2O$	5	1.6	TGA PXRD	Water vapor	[11]
$Eu_3(H_{0.75}O_3PCHOHCOO)_4\cdot xH_2O$	10	2	Decay time Emission spectra	Water vapor	[12]
$[Tb(L2)(C_2H_2O_4)_{0.5}(H_2O)]_2\cdot H_2O$	60	24	Emission spectra	Ambient conditions	[13]
$[Eu_2(CO_3)(ox)_2(H_2O)_2]\cdot 4H_2O$	n.d.	12	PXRD	90% Relative Humidity	[14]
$\{[Eu_2(L3)_2]\ (H_2O)_3(Me_2NH_2)_2\}_n$	n.d.	48	PXRD	Refluxed in water	[15]
$\{[Tb_4(OH)_4(DSOA)_2(H_2O)_8]\cdot(H_2O)_8\}_n$	n.d.	24	PXRD	Boiling water	[16]

Abbreviations: mpca = 2-pyrazine-5-methyl-carboxylate; fum = fumarate dianion; L1 = 4,4′-disulfo-2,2′-bipyridine N,N′-dioxide; BDOA = benzene-1,4-dioxylacetate; bpy = 2,2'-bipyridine; ip = isophthalate; ox = oxalate; bdc = benzene-1,2-dicarboxylate; 2,5-pydc = 2,5-pyridinedicarboxylate; HPA = 2-hydroxyphosphonoacetate; L2 = pyridyl-4,5-imidazole dicarboxylate; L3 = 5-(3,5-dicarboxybenzyloxy)-isophthalate; DSOA = disodium-2,2′-disulfonate-4,4′-oxydibenzoicate; n. d. = not determined.

References

1. S. Tanase, F. Prins, J. M. M. Smits and R. de Gelder, *CrystEngComm*, 2006, **8**, 863.
2. S. Tanase, M. C. Mittelmeijer-Hazeleger, G. Rothenberg, C. Mathonière, V. Jubera, J. M. M. Smits and R. de Gelder, *Journal of Materials Chemistry*, 2011, **21**, 15544.
3. Y. Gao, R. Broersen, W. Hageman, N. Yan, M. C. Mittelmeijer-Hazeleger, G. Rothenberg and S. Tanase, *J. Mater. Chem. A*, 2015, **3**, 22347.
4. A. Michaelides, S. Skoulika, E. G. Bakalbassis and J. Mrozinski, *Cryst. Growth Des.*, 2003, **3**, 487.
5. D. T. C. Brett D. Chandler, and George K. H. Shimizu, *J. Am. Chem. Soc.*, 2006, 10403.
6. Y.-Z. L. Xian-Lan Hong, Huaimin Hu, Yi Pan, Junfeng Bai and Xiao-Zeng You, *Cryst. Growth Des.*, 2006, **6**, 1221.
7. W. H. Zhu, Z. M. Wang and S. Gao, *Dalton Trans.*, 2006, 765.
8. F. Luo, S. R. Batten, Y. Che and J. M. Zheng, *Chem. Eur. J.*, 2007, **13**, 4948.
9. P. M. a. S. Natarajan, *Inorg.Chem.*, 2007, 1250.
10. Z.-M. W. Wen-Hua Zhu, and Song Gao, *Inorg. Chem.*, 2007, **4**, 1338.
11. P. Mahata, K. V. Ramya and S. Natarajan, *Inorg. Chem.*, 2009, **48**, 4942.
12. R. M. P. Colodrero, K. E. Papathanasiou, N. Stavgianoudaki, P. Olivera-Pastor, E. R. Losilla, M. A. G. Aranda, L. León-Reina, J. Sanz, I. Sobrados, D. Choquesillo-Lazarte, J. M. García-Ruiz, P. Atienzar, F. Rey, K. D. Demadis and A. Cabeza, *Chem. Mater.*, 2012, **24**, 3780.
13. Y. Yu, J.-P. Ma and Y.-B. Dong, *CrystEngComm*, 2012, **14**, 7157.
14. Q. Tang, Y. Liu, S. Liu, D. He, J. Miao, X. Wang, G. Yang, Z. Shi and Z. Zheng, *J. Am. Chem. Soc.*, 2014, **136**, 12444.
15. R. Wang, X. Y. Dong, H. Xu, R. B. Pei, M. L. Ma, S. Q. Zang, H. W. Hou and T. C. Mak, *Chem. Commun.*, 2014, **50**, 9153.
16. H. Y. Li, H. Xu, S. Q. Zang and T. C. Mak, *Chem. Commun.*, 2016, **52**, 525.